

## Thermal buckling of functionally graded plates

Thamires X. Cavalcante<sup>1</sup>, Evandro Parente Jr.<sup>1</sup>, Marcelo S. Medeiros Junior<sup>1</sup>

<sup>1</sup>*Department of Structural Engineering and Civil Construction, Federal University of Ceara  
Campus do Pici, Technology Center, Block 728, 60455-760, Fortaleza, CE, Brazil  
thamiresximenes@alu.ufc.br; evandro@ufc.br; marcelomedeiros@ufc.br*

**Abstract.** Plates and shells are widely used in several areas, such as civil construction, automotive, aerospace, naval, and defense industries. The application of Functionally Graded Materials (FGM) in plate and shell structures can provide several benefits. FGMs are composed by two or more materials, in which the microstructure changes continuously and smoothly from one surface to another, being designed to achieve the desired properties according to the application of interest. The most common are those composed of ceramic and metallic materials, used for example in structures subjected to high temperatures used in the aerospace industry. The structures of plates and shells can be highly slender, becoming sensitive to collapse due to buckling. Thus, this study focuses on the analysis of FGM plates stability at high temperatures, evaluating the influence of the slenderness and the volume fraction distribution in the critical temperature and post-critical behavior. The numerical simulations of the FGM structures are performed using the commercial *software* Abaqus. To correctly represent the thermomechanical behavior of functionally graded materials, the Virtual Lamina Method (VLM) for buckling and user material subroutines (UMATs) for post-buckling are applied.

**Keywords:** Stability, FGM, Thermal Loading, Finite Element Method.

### 1 Introduction

Plates and shells are widely used in various fields, as civil construction, automotive, aerospace, marine, and defense industries. In addition to mechanical loading, these structures in service can be subjected to high thermal loads, as in the case of aerospace structures. Aiming the development of heat shields for space reentry, scientists in Japan introduced the concept of materials with functional gradation, aerospace scientists in Japan in 1984 introduced the concept of materials with functional gradation [1].

Functionally Graded Materials (FGMs) are composites whose mechanical properties vary continuously and smoothly from one surface to another, avoiding stress concentrations and reducing residual stresses [2]. The most common FGMs are composed of ceramic and metallic materials. Ceramic has good capacity to withstand high temperatures and metal has good strength and fracture toughness [3].

Several works were developed for the analysis of functionally graded plates and shells. Reddy and Chin [4] developed a study aimed at the dynamic thermoelastic analysis of cylinders and plates with functional gradation, proposing a finite element formulation, that taking into account the thermomechanical coupling. Kordkheili and Naghdabadi [5] performed a nonlinear analysis of the static thermoelastic behavior for FGM composite plates and shells, applying the updated Lagrangian approach.

Alijani *et al.* [6] studied the thermal effects on nonlinear vibrations of double curvature shells with functional gradation, applying higher order shear strain theory. The buckling and post-buckling analysis of FGM plates and shells under thermal loading using the Finite Element Method (FEM) were developed in the works of Na and Kim [7–9], Trabelsi *et al.* [10] and Moita *et al.* [11]. Along the same lines, other works were developed using Isogeometric Analysis (IGA), such as the one by Tran *et al.* [12], Babaei *et al.* [13] and Rezaiee-Pajand *et al.* [14]. Shen and the other coauthors developed several studies on the post-buckling behavior of a cylindrical shell in thermal environments [3, 15–19].

Plates and shells are susceptible to collapse from of stability, due to their high slenderness. When subjected to high temperatures, the material undergoes thermal expansion, in cases where displacements are restricted causing

compressive stress, the structure may suffer an elastic instability, known as thermal buckling [20].

Thus, it is necessary to develop studies concerning of thermal stability in functionally graded plates. In this context, this work aims to present a methodology for thermal buckling analysis of FGMs in plate structures using FEM. Including the determination of critical temperature, buckling modes and post-critical path and the influence of volume fraction distribution and length to thickness ratio ( $a/h$ ). The computer simulations were performed in the commercial *software* Abaqus. The Virtual Lamina Method (VLM) was applied to correctly represent the thermomechanical behavior of FGMs for buckling and user material subroutines (UMATs) for post-buckling.

## 2 Functionally graded materials

FGMs are composites formed by two or more materials, whose composition varies in a continuous and smooth way along the structure. In the case of plates and shells, the volume fractions distribution can be defined according to the power law:

$$V_m = \left(0.5 - \frac{z}{h}\right)^N, \quad V_c + V_m = 1 \quad (1)$$

where,  $z$  is the coordinate in which the properties changes,  $h$  is the total thickness of the plate or shell,  $N$  corresponds to the fraction index of volume,  $V_m$  and  $V_c$  correspond to the volume of metal and ceramic, respectively. Fig.1 presents a graph with the variation of the metal volume fraction along the thickness in relation to the volume fraction index, according to the power law.

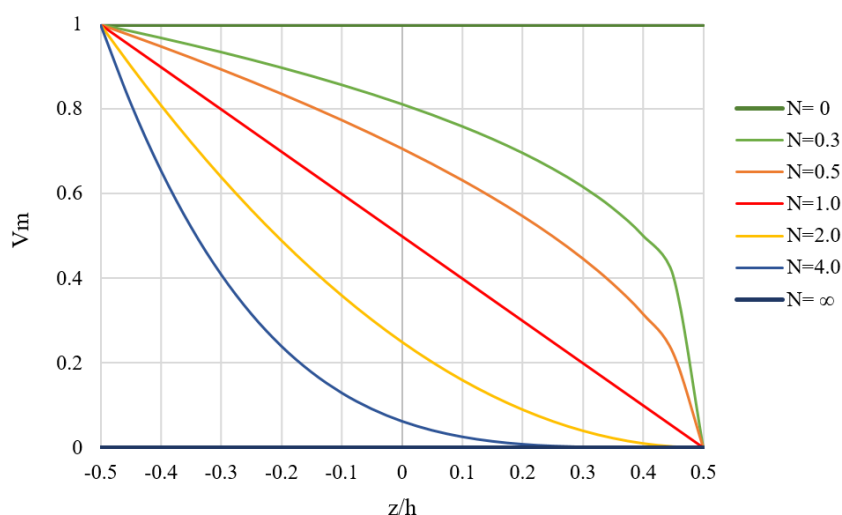


Figure 1. Variation of volume fraction  $V_m$ .

Effective material properties are obtained through the application of homogenization techniques. The most used are the law of mixtures (Voigt) and Mori-Tanaka [21]. In this study, the first methodology is applied, in which the effective properties ( $P_{eff}$ ) of the composite are calculated as:

$$P_{eff}(z) = P_m V_m(z) + P_c(1 - V_m(z)) \quad (2)$$

where,  $P_m$  and  $P_c$  correspond to the properties of metal and ceramic, respectively.

## 3 Finite Element Method

In the incremental finite element formulation for nonlinear analysis, the displacement vector ( $\mathbf{u}$ ), stress ( $\mathbf{S}$ ) and strain ( $\mathbf{E}$ ) in the increment to be calculated are expressed by [9]:

$$\mathbf{u} = \mathbf{u}^{(i)} + \Delta \mathbf{u} \quad (3)$$

$$\mathbf{S} = \mathbf{S}^{(i)} + \Delta \mathbf{S} \quad (4)$$

$$\mathbf{E} = \mathbf{E}^{(i)} + \Delta \mathbf{E} = \mathbf{E}^{(i)} + \Delta \varepsilon + \Delta \eta \quad (5)$$

where  $\Delta \varepsilon$  and  $\Delta \eta$  represent the linear and nonlinear incremental strain vectors in  $\Delta \mathbf{u}$ . Note that the (i) superscript symbology is used to represent the initial values and  $\Delta$  the incremental ones. The equilibrium equation is given by:

$$\int_V \delta \mathbf{E}^T \mathbf{S}^T dV - \delta W = 0 \quad (6)$$

where,  $\delta W$  is the work of external forces. Replacing the Eq.(3)-(5), we have:

$$\int_V \delta \varepsilon^T \Delta \mathbf{S}^T dV + \int_V \delta \varepsilon^{T(i)} \mathbf{S} dV + \int_V \delta \eta^{T(i)} \mathbf{S} dV - \delta W = 0 \quad (7)$$

The incremental strain vector and the virtual strain vector work are given by:

$$\Delta \varepsilon = \mathbf{B} \Delta \mathbf{u}_e, \quad \delta \varepsilon = \mathbf{B} \delta \mathbf{u}_e \quad (8)$$

where,  $\mathbf{B}$  corresponds to the matrix of the derivatives of the shape functions and  $\Delta \mathbf{u}_e$  referring to the nodal degrees of freedom of the incremental element. The stress vector  $\mathbf{S}^{(i)}$  and the increment of the stress vector are formulated by:

$$\mathbf{S}^{(i)} = \mathbf{C}(\mathbf{E}^{(i)} - \mathbf{E}^{(th)}), \quad \Delta \mathbf{S} = \mathbf{C} \Delta \varepsilon \quad (9)$$

where,  $\mathbf{C}$  is the matrix of elastic constants and  $\mathbf{E}^{(th)}$  the vector of thermal deformations, obtained by:

$$\mathbf{E}^{(th)} = \Delta T [\alpha \quad \alpha \quad \alpha \quad 0 \quad 0 \quad 0]^T \quad (10)$$

Finally, the linearized equilibrium equation can be achieved by substituting Eq.(8)-(10) in Eq.(7).

$$\sum_e \delta \mathbf{u}_e^T [(\mathbf{K}_l + \mathbf{K}_s)] \Delta \mathbf{u}_e - (\mathbf{Q}_{el} + \mathbf{Q}_{th} - \mathbf{Q}^{(i)}) = 0 \quad (11)$$

where,  $\mathbf{K}_l$  and  $\mathbf{K}_s$  correspond to the linear stiffness matrix and the stiffness matrix generated by the stresses of the (i)th step.  $\mathbf{Q}$  refer to the element's nodal charge vectors,  $\mathbf{Q}^{(i)}$  due to the stress in the (i) th state,  $\mathbf{Q}_{th}$  generated by the deformation thermally induced and  $\mathbf{Q}_{el}$  is the element's nodal load vector due to the applied loads. Being expressed by:

$$\mathbf{Q}^{(i)} = \int \mathbf{B}^T \mathbf{C}^{(i)} \mathbf{E} dV_e \quad (12)$$

$$\mathbf{Q}_{th} = \int \mathbf{B}^T \mathbf{C} \mathbf{E}^{th} dV_e \quad (13)$$

Performing the assembly process, we obtain:

$$\delta \mathbf{u}^T (\mathbf{K} \Delta \mathbf{u} - \Delta \mathbf{Q}) = 0 \quad (14)$$

where,  $\delta \mathbf{q}$  the vector of the global incremental nodal degrees of freedom,  $\mathbf{K}$  is the global tangent stiffness matrix and  $\Delta \mathbf{Q}$  the charge vector global incremental nodal. Finally, write:

$$\mathbf{K} \Delta \mathbf{u} = \Delta \mathbf{Q} \quad (15)$$

The trace of the equilibrium path can be determined by several methods such as Displacement Control, Load Control, Arc-length and others. The Arc-length method is the most used since it can trace the nonlinear equilibrium path of structures presetting limit points and snap-backs. However, it needs smaller increments for convergence.

### 3.1 Thermal buckling

When the structure is subjected to thermal gradients, the material undergoes thermal expansion, in cases where displacements are restricted, causing compression stress, the structure may suffer loss of stability, in this case known as thermal buckling. The critical temperature value can be obtained by solving the eigenvalue problem:

$$(\mathbf{K}_L + \lambda \mathbf{K}_S) \mathbf{u}^D = 0 \quad (16)$$

where,  $\lambda$  is the eigenvalue,  $\mathbf{u}^D$  the associated mode,  $K_L$  and  $K_S$  correspond to the global linear stiffness matrix and the stress matrix global, respectively. Finally, the critical temperature is obtained by:

$$T_{cr} = \lambda_{cr} \Delta T + T_{ref} = \Delta T_{cr} + T_{ref} \quad (17)$$

where,  $\lambda_{cr}$  is the smallest eigenvalue,  $\Delta T_{cr}$  is the critical temperature variation and  $T_{ref}$  corresponds to the reference temperature. The equilibrium path is obtained by solving Eq.(15), applying the critical temperature and its associated mode.

## 4 Numerical results and discussions

A rectangular plate made out of Alumina and Nickel and with all four edges clamped, will be analyzed. The material properties are shown in Tab. 1. The structure is subjected to a uniform temperature rise with a reference temperature of 290K.

Table 1. Material properties

	<i>Al<sub>2</sub>O<sub>3</sub></i>	<i>Ni</i>
Modulus of elasticity (GPa)	393.00	199.50
Poisson's ratio	0.25	0.30
Coefficient of thermal expansion (°C <sup>-1</sup> × 10 <sup>-6</sup> )	8.80	13.30

It is worth noting that the modeling of FGM structures can be performed through the use of user material subroutines (UMAT). However, this methodology has some limitations in ABAQUS, for example, in determining the critical temperature by means of BUCKLE analysis step. In cases like this, the Virtual Lamina Method (VLM)

can be applied, in which the structure is divided into a set of layers, where each layer is considered as isotropic material, the properties of which correspond to the values of the central coordinates of each layer.

The subdivision of the structure was carried out using VLM, the S8R element and a 10x10 element mesh. The number of virtual layers needed for the simulations was evaluated by comparing them with the critical load values for  $a/h = 50$  and  $N = 1$ , present in [7, 9], respectively 121.53 and 121.48 . The results presented in Tab. 2, show that the use of 10 layers leads to satisfactory results. Thus, the simulations use 10 virtual layers.

Table 2. Critical temperature ( $a/h = 50$  e  $N = 1$ )

Number of layers	Critical temperature range
5	121.90
10	121.73
15	121.69

Through the graph shown in Fig. 2, it is observed that the critical temperature variation of the plate undergoes a sharp decrease as the aspect ratio  $a/h$  of the structure increases. In relation to the volume fraction index, there is an increase in the critical variation with its increase, since the increase in  $N$  indicates the increase in the ceramic volume.

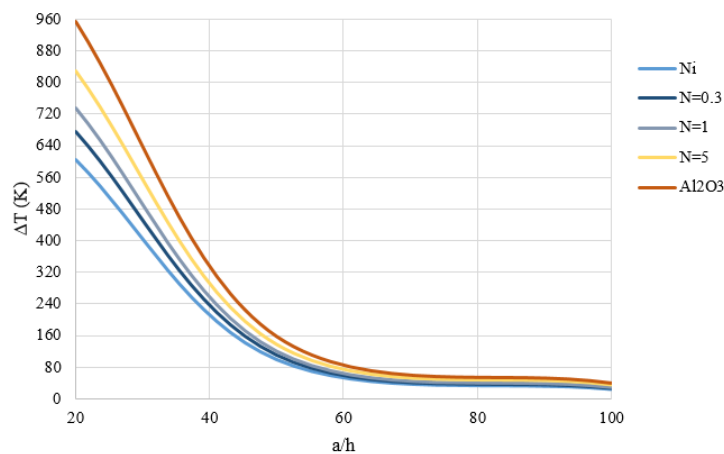


Figure 2. Critical temperature range

Fig.3 presents the four initial buckling modes. It is noteworthy that the important thing for design is the first critical mode, in which the structure loses stability.

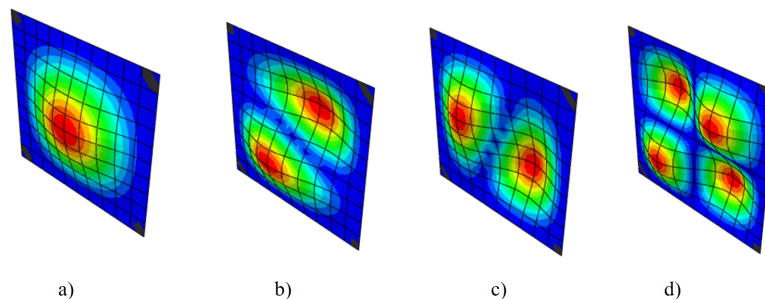


Figure 3. Buckling modes: a) 1st, b) 2nd, c) 3rd and d) 4th mode

To perform the post-critical path tracing, a point load was inserted in the center of the plate, this procedure is adopted in order to generate a small imperfection from the load application. A UMAT subroutine created in Fortran and coupled with ABAQUS was applied. The mesh used was 10x10x10 with application of the 3D element C3D20R.

Fig.4 shows the post-buckling behavior due to a uniform temperature increase for different  $a/h$  ratios, assuming  $N = 1$ . The values obtained in the simulations are compared with those presented in Trabelsi *et al.* [10]. In addition to the reduction in critical variation with the increase in the  $w/h$  ratio, there is an increase in the central displacement of the plate. It is verified that the post-buckling path is given by stable bifurcation, in which the plate is able to withstand temperatures higher than the critical one.

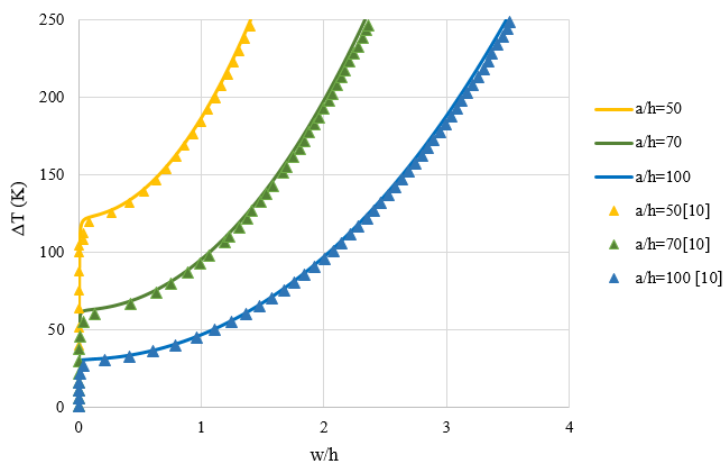


Figure 4. Post-critical path for  $N = 1$

Fig.5 shows the equilibrium path for a uniform temperature increase for different values of  $N$ . It can be seen that the maximum displacement of the FGM plate is smaller than the one composed by only metal and larger than the than the all-ceramic plate. As the volume of metal increases the displacement increases for the same temperature. It is noteworthy that both graphs of the equilibrium path showed good agreement with those presented by Trabelsi *et al.*[10].

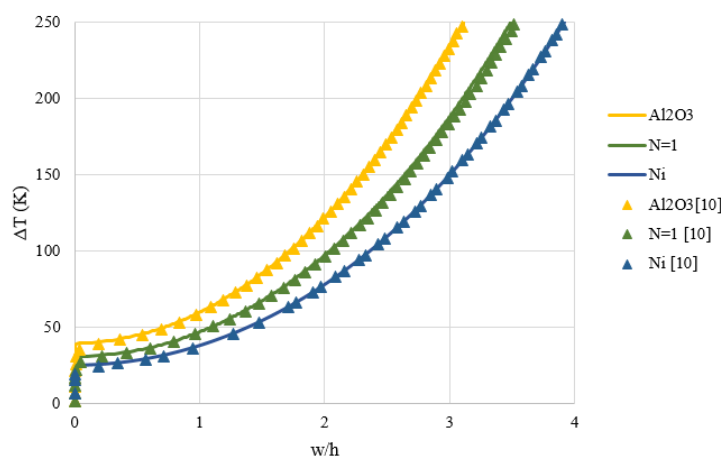


Figure 5. Post-critical path for  $a/h = 100$

## 5 Conclusion

This work dealt with the thermal buckling analysis of FGM plates using FEM, applying VLM for buckling and UMATs for post-buckling. It is noteworthy that this methodology can also be applied to shells. Note that as the geometric parameter  $a/h$  increases, the critical temperature gradient decreases considerably. Thus, the thinner the plate, the smaller the critical variation required for thermal buckling to occur. Regarding the volume fraction index, it is observed that the higher the value of  $N$ , the smaller the displacements and the greater the critical temperature variation.

**Acknowledgements.** The authors are grateful for the financial support of the Fundação Cearense de Apoio ao Desenvolvimento Científico e Tecnológico (FUNCAP).

**Authorship statement.** The authors hereby confirm that they are the sole liable persons responsible for the authorship of this work, and that all material that has been herein included as part of the present paper is either the property (and authorship) of the authors, or has the permission of the owners to be included here.

## References

- [1] M. Koizumi. Fgm activities in japan. *Composites Part B: Engineering*, vol. 28, n. 1-2, pp. 1–4, 1997.
- [2] S. Akavci. Thermal buckling analysis of functionally graded plates on an elastic foundation according to a hyperbolic shear deformation theory. *Mechanics of Composite Materials*, vol. 50, n. 2, pp. 197–212, 2014.
- [3] H.-S. Shen. *Functionally graded materials: nonlinear analysis of plates and shells*. CRC press, 2016.
- [4] J. Reddy and C. Chin. Thermomechanical analysis of functionally graded cylinders and plates. *Journal of thermal Stresses*, vol. 21, n. 6, pp. 593–626, 1998.
- [5] S. Hosseini Kordkheili and R. Naghdabadi. Geometrically non-linear thermoelastic analysis of functionally graded shells using finite element method. *International journal for numerical methods in Engineering*, vol. 72, n. 8, pp. 964–986, 2007.
- [6] F. Alijani, M. Amabili, and F. Bakhtiari-Nejad. Thermal effects on nonlinear vibrations of functionally graded doubly curved shells using higher order shear deformation theory. *Composite Structures*, vol. 93, n. 10, pp. 2541–2553, 2011.
- [7] K.-S. Na and J.-H. Kim. Three-dimensional thermomechanical buckling of functionally graded materials. *AIAA journal*, vol. 43, n. 7, pp. 1605–1612, 2005.
- [8] K.-S. Na and J.-H. Kim. Nonlinear bending response of functionally graded plates under thermal loads. *Journal of Thermal Stresses*, vol. 29, n. 3, pp. 245–261, 2006a.
- [9] K.-S. Na and J.-H. Kim. Thermal postbuckling investigations of functionally graded plates using 3-d finite element method. *Finite Elements in Analysis and Design*, vol. 42, n. 8-9, pp. 749–756, 2006b.
- [10] S. Trabelsi, A. Frikha, S. Zghal, and F. Dammak. Thermal post-buckling analysis of functionally graded material structures using a modified fsdt. *International Journal of Mechanical Sciences*, vol. 144, pp. 74–89, 2018.
- [11] J. S. Moita, A. L. Araújo, V. F. Correia, C. M. M. Soares, and J. Herskovits. Buckling and nonlinear response of functionally graded plates under thermo-mechanical loading. *Composite Structures*, vol. 202, pp. 719–730, 2018.
- [12] L. V. Tran, P. Phung-Van, J. Lee, M. A. Wahab, and H. Nguyen-Xuan. Isogeometric analysis for nonlinear thermomechanical stability of functionally graded plates. *Composite Structures*, vol. 140, pp. 655–667, 2016.
- [13] H. Babaei, Y. Kiani, and M. Eslami. Geometrically nonlinear analysis of functionally graded shallow curved tubes in thermal environment. *Thin-Walled Structures*, vol. 132, pp. 48–57, 2018.
- [14] M. Rezaiee-Pajand, D. Pourhekmatt, and E. Arabi. Thermo-mechanical stability analysis of functionally graded shells. *Engineering Structures*, vol. 178, pp. 1–11, 2019.
- [15] H.-S. Shen. Postbuckling analysis of axially-loaded functionally graded cylindrical shells in thermal environments. *Composites Science and Technology*, vol. 62, n. 7-8, pp. 977–987, 2002.
- [16] H.-S. Shen. Postbuckling analysis of pressure-loaded functionally graded cylindrical shells in thermal environments. *Engineering Structures*, vol. 25, n. 4, pp. 487–497, 2003.
- [17] H.-S. Shen and N. Noda. Postbuckling of fgm cylindrical shells under combined axial and radial mechanical loads in thermal environments. *International Journal of Solids and Structures*, vol. 42, n. 16-17, pp. 4641–4662, 2005.
- [18] H.-S. Shen and N. Noda. Postbuckling of pressure-loaded fgm hybrid cylindrical shells in thermal environments. *Composite structures*, vol. 77, n. 4, pp. 546–560, 2007.
- [19] H.-S. Shen and H. Wang. Thermal postbuckling of fgm cylindrical panels resting on elastic foundations. *Aerospace Science and Technology*, vol. 38, pp. 9–19, 2014.
- [20] da R. Silva Michaello, J. R. S. Paes, L. A. Isoldi, R. G. Bastos, dos E. D. Santos, and L. A. O. Rocha. Perfis perfurados submetidos à flambagem térmica e mecânica. *Exatas & Engenharias*, vol. 8, n. 20, 2018.
- [21] H.-S. Shen and Z.-X. Wang. Assessment of voigt and mori–tanaka models for vibration analysis of functionally graded plates. *Composite Structures*, vol. 94, n. 7, pp. 2197–2208, 2012.